XL CILAMCE
IBERO-LATIN AMERICAN CONGRESS ON COMPUTATIONAL METHODS IN ENGINEERING
NOVEMBER 11-14, 2019
Praiamar Natal Hotel & Convention Natal, RN-BRAZIL

AN EFFECTIVE BEM/FEM FORMULATION FOR THE STATIC INTERACTION ANALYSIS OF PILE GROUPS EMBEDDED IN A SEMI-INFINITE CONTINUUM

Endi S. Luamba
Ray C.S. Silva
luamba@usp.br
raycalazans@usp.br
São Carlos School of Engineering, University of São Paulo
Av. Trabalhador São-carlense, 400, 13566-590, São Carlos/SP, Brazil
Ana P.F. Ramos
ramosapf@gmail.com
Caraúbas Campus, Federal University of the Semi-Arid Region
Av. Universitária "Leto Fernandes", Sítio Esperança II, 59780-000, Caraúbas/RN, Brazil
João B. de Paiva
paiva@sc.usp.br
São Carlos School of Engineering, University of São Paulo
Av. Trabalhador São-carlense, 400, 13566-590, São Carlos/SP, Brazil

Abstract. In the literature, numerical analysis of pile–soil interaction is performed by a variety of formulations based on Finite Element Method (FEM), Finite Difference Method (FDM), Boundary Element Method (BEM) or a combination of two numerical methods. In those formulations, very complex and computationally expensive meshes are generally used. In this paper, pile–soil interaction problems are solved with relatively simple and yet efficient meshes as a result of coupling the BEM with the FEM, and using Mindlin's fundamental solution for the soil modeling. To adequately consider the flexibility of the pile, the same is discretized into a parametric number of three-dimensional finite beam elements. Therefore, the pile can be of any size and subjected to any type of loading including axial, lateral and moment loads. Moreover, the formulation can be easily extended so that a foundation plate can be coupled to piles to form a capped pile group or a piled raft. The efficiency of the developed and implemented formulations is properly demonstrated through numerical examples including single piles and pile groups.

Keywords: Pile–soil interaction, Boundary element, Finite element, Pile groups, Coupled analysis

1 Introduction

Pile foundations are generally used for large structures to satisfy the allowable settlement. They provide reinforcement to the soil, increasing its load capacity and modifying its deformation behavior. In practice, there are few problems that can be solved analytically. Most real engineering problems, such as the ones involving soil–structure interaction, are too complex to be solved by analytical methods. Analytical formulations are generally applicable to problems whose required assumptions simplify much the actual physical phenomenon, and to problems with simple geometries and boundary conditions. However, one of the important applications of analytical solutions is to validate limit cases of numerical models, and promote the development of more robust numerical methods.

The resolution of very complex boundary value problems is thence made via numerical methods such as the Boundary Element Method (BEM) and the Finite Element Method (FEM). Experimental analysis can also be carried out but a numerical method is generally preferred as a first approach to obtain preliminary results or as the unique approach for the entire analysis. Experimental results may only apply to one situation and may be costly, difficult or time-consuming to replicate. For the pile–soil interaction problem, an example of an experimental analysis is by Kérisel and Adam [1] about lateral displacements of a driven pile embedded in a clay layer.

In the literature, there are numerous numerical approaches for the static analysis of pile-soil interaction problems. In Helwany [2] there is a chapter dedicated to the analysis of single piles and pile groups using analytical and numerical methods. The traditional FEM is used in the modeling of the pile-soil assembly. The Kelvin's fundamental solution is used in Ribeiro and Paiva [3] in the modeling of the soil and infinite boundary elements are required in order to increase the accuracy of the results. In Parreira and Varatojo [4], the BEM is used for the modeling of the pile-soil assembly, with the implementation of infinite boundary elements for representing layered domains by subregions. A general shortcoming of those formulations is the complex meshes required in the problem modeling.

In the present study, these same problems are analyzed combining the BEM and the FEM, resulting in very practical meshes. The analysis may also be completely performed using only the FEM. However, coupling the BEM and the FEM has the advantage of considerably reducing the degrees of freedom of the model, hence, saving on computational costs. Moreover, one of the special features of the BEM (Aliabadi [5]) is the automatic satisfaction of boundary conditions for infinite and semi-infinite regions, thus avoiding the numerical approximation of remote boundaries.

In a previous study by Luamba and Paiva [6] only one pile was considered and subjected to a lateral load. In the present formulation, single piles and pile groups are analyzed, and are subjected to axial, lateral and moment loads. The spacing between the piles is taken as the distance between the axes. A rough contact is assumed along the interface region between the piles and the soil. The pile is modeled by the FEM and discretized by a parametric number of three-dimensional finite beam elements. The interaction tractions along every finite element have a linear distribution. The flexibility of the pile is well considered since a sufficient number of finite elements are used for its discretization.

The soil considered as semi-infinite, homogeneous, isotropic and linear elastic continuum, is modeled by the BEM using Mindlin's fundamental solution [7]. This fundamental solution is especially appropriate for models containing semi-infinite solids, inasmuch as only the line loads need to be discretized, and not all the three-dimensional soil's model. Therefore, the unknown variables, and consequently the dimensions of the matrices involved, the processing time and the modeling complexity, are considerably reduced. Moreover, contrary to the formulations by Poulos and Davis [8] and Ai et al. [9], the present formulation can be easily extended for a full plate–pile–soil interaction since the displacements and rotations at the top of the pile appear as unknowns in the system of equations.

The governing equations are obtained combining the soil equations from the BEM and the pile equations from the FEM taking into account the force equilibrium and the displacement compatibility that must hold along the interface between the pile and the soil. The final system is therefore composed by an equivalent stiffness matrix, a vector of the applied loads at the top of the piles and a

vector of the nodal displacements and rotations. Numerical examples of pile–soil interaction problems are solved and the results obtained are highly consistent with those from other formulations.

2 Pile equations

The pile is discretized by a parametric number of three-dimensional finite beam elements. The elements are linear and each node has five DOFs (degrees of freedom), as shown in Fig. 1. At the top of the pile, horizontal forces H_x and H_y, vertical force V, and bending moments M_x and M_y, may be applied.

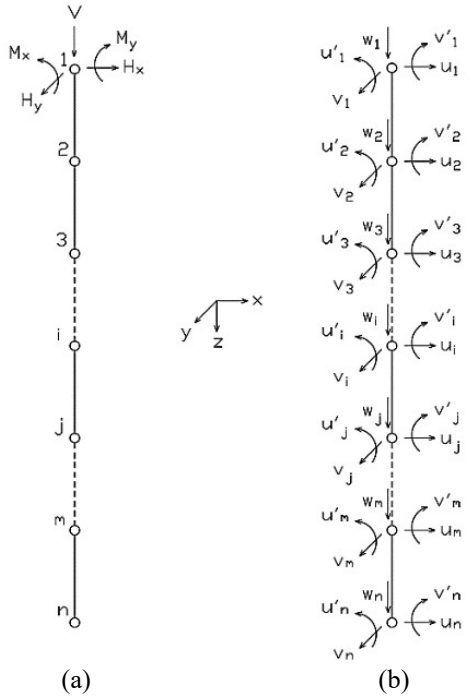

(a) (b)

Figure 1. Pile modeling: (a) applied loads and (b) nodal parameters.

The DOFs at each node are: horizontal displacements u and v, vertical displacement w, and rotations u' and v' around the y-axis and the x-axis, respectively.

$$\{u\}_e^T = \{u_i \;\; v_i \;\; w_i \;\; u_i' \;\; v_i' \;\; u_j \;\; v_j \;\; w_j \;\; u_j' \;\; v_j'\}. \tag{1}$$

$\{u\}_e^T$ is the vector of nodal displacements for the finite element e delimited by nodes i and j.

The total potential energy of the pile Π is used in order to determine its stiffness matrix:

$$\Pi = U + \Omega. \tag{2}$$

U is the potential energy of deformation or the elastic potential energy of the pile and Ω is the potential energy of the applied loads.

For a pile of length L and modelled as shown in Fig. 1, U and Ω are given by:

$$U = \frac{EI}{2}\int_0^L u''^2 dz + \frac{EI}{2}\int_0^L v''^2 dz + \frac{EA}{2}\int_0^L w'^2 dz, \tag{3}$$

$$\Omega = -H_x\bar{u} - H_y\bar{v} - V\bar{w} - M_x\bar{u}' - M_y\bar{v}' + \int_0^L Q_x(z)u(z)dz + \int_0^L Q_y(z)v(z)dz + \int_0^L Q_z(z)w(z)dz. \tag{4}$$

E is the Young's modulus of the pile, I is the area moment of inertia of the pile cross-section ($I = I_x = I_y$), A is the pile cross-section area, Q_x, Q_y, Q_z are the interface tractions along the pile, and u_x, u_y, u_z are the displacements of the node at the top of the pile.

The total potential energy Π has to be minimized for obtaining the equilibrium condition. Therefore, the following system of equations is obtained:

$$[K]\{u\} = \{F\} + [T]\{Q\}. \tag{5}$$

$[K]$ is the stiffness matrix of the pile, $\{u\}$ is the vector of nodal displacements of the pile given by: $\{u\}^T = \{u_1 \;\; v_1 \;\; w_1 \;\; u_1' \;\; v_1' \;\; u_2 \;\; v_2 \;\; w_2 \;\; u_2' \;\; v_2' \ldots \; u_n \;\; v_n \;\; w_n \;\; u_n' \;\; v_n'\}$, $\{F\}$ is the vector of the external forces applied to the top of the pile given by: $\{F\} = \{H_x \;\; H_y \;\; V \;\; M_x \;\; M_y \;\; 0 \;\; 0 \;\; 0 \;\; 0 \;\; 0 \ldots \; 0 \;\; 0 \;\; 0 \;\; 0 \;\; 0\}$, $[T]$ is the matrix that transforms pile–soil interface tractions into equivalent nodal forces, and $\{Q\}$ is the vector of pile–soil interface tractions.

For a single finite element e of the pile, the stiffness matrix $[K]^e$ is given by:

$$[K]^e = \int_0^L [B]^T EI\,[B]\,dz. \tag{6}$$

EI is the bending rigidity of the element and $[B]$ is the strain-displacement interpolation matrix.

$$[K]^e = \begin{bmatrix} \frac{12EI}{L^3} & 0 & 0 & \frac{6EI}{L^2} & 0 & -\frac{12EI}{L^3} & 0 & 0 & \frac{6EI}{L^2} & 0 \\ 0 & \frac{12EI}{L^3} & 0 & 0 & \frac{6EI}{L^2} & 0 & -\frac{12EI}{L^3} & 0 & 0 & \frac{6EI}{L^2} \\ 0 & 0 & \frac{EA}{L} & 0 & 0 & 0 & 0 & -\frac{EA}{L} & 0 & 0 \\ \frac{6EI}{L^2} & 0 & 0 & \frac{4EI}{L} & 0 & -\frac{6EI}{L^2} & 0 & 0 & \frac{2EI}{L} & 0 \\ 0 & \frac{6EI}{L^2} & 0 & 0 & \frac{4EI}{L} & 0 & -\frac{6EI}{L^2} & 0 & 0 & \frac{2EI}{L} \\ -\frac{12EI}{L^3} & 0 & 0 & -\frac{6EI}{L^2} & 0 & \frac{12EI}{L^3} & 0 & 0 & -\frac{6EI}{L^2} & 0 \\ 0 & -\frac{12EI}{L^3} & 0 & 0 & -\frac{6EI}{L^2} & 0 & \frac{12EI}{L^3} & 0 & 0 & -\frac{6EI}{L^2} \\ 0 & 0 & -\frac{EA}{L} & 0 & 0 & 0 & 0 & \frac{EA}{L} & 0 & 0 \\ \frac{6EI}{L^2} & 0 & 0 & \frac{2EI}{L} & 0 & -\frac{6EI}{L^2} & 0 & 0 & \frac{4EI}{L} & 0 \\ 0 & \frac{6EI}{L^2} & 0 & 0 & \frac{2EI}{L} & 0 & -\frac{6EI}{L^2} & 0 & 0 & \frac{4EI}{L} \end{bmatrix}. \tag{7}$$

3 Soil equations

The soil is modeled with line loads at the same location of the piles, and using the same discretization. The source points (s) and the field points (f) are placed along the line loads so that the matrix $[G]$ of the soil's influence coefficients can be determined. A numerical integration is performed using Gauss integral points. The equilibrium of the continuum is obtained by the Somigliana identity which is a boundary integral equation given by:

$$C(s)u(s) + \int_{\Gamma} P^*(s,f)u(f)d\Gamma = \int_{\Gamma} u^*(s,f)P(f)d\Gamma + \int_{\Omega} u^*(s,f)b(f)d\Omega\,. \tag{8}$$

The pile is embedded in a homogenous, isotropic and linear elastic semi-infinite continuum, with interface tractions Q acting along its depth and the stress σ_b is uniformly distributed at the base of the pile, as shown in Fig. 2. Therefore, Eq. (8) is rewritten as:

$$\begin{aligned} C(s)\,u(s) + \int_{\Gamma} P^*(s,f)\,u(f)\,d\Gamma = \int_{\Gamma} u^*(s,f)\,P(f)\,d\Gamma + \int_{\Omega} u^*(s,f)\,b(f)\,d\Omega + \\ + \int_{\Gamma_q} u^*(s,f)\,Q(f)\,d\Gamma_q + \int_{\Gamma_b} u^*(s,f)\,\sigma_b(f)\,d\Gamma_b\,. \end{aligned} \tag{9}$$

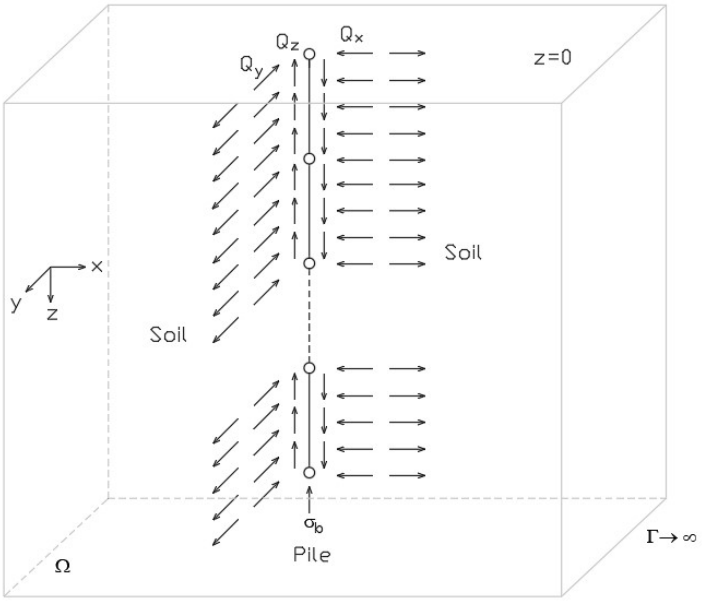

Figure 2. Interface tractions acting along the pile and in the soil domain.

Mindlin's fundamental solution for displacements $u^*(s,f)$ is used and the volumetric forces are neglected. The pile domain coincides with the pile boundary Γ_q and $C(s)$ is equal to the identity matrix. Therefore, Eq. (9) becomes:

$$u(s) = \sum_{i=1}^{N_p} \left[\int_{\Gamma_{q_i}} u^*(s,f)Q(f)d\Gamma_{q_i} + \int_{\Gamma_{b_i}} u^*(s,f)\sigma_b(f)d\Gamma_{b_i} \right]. \tag{10}$$

N_p is the number of line loads and it is equal to the number of piles embedded in the semi-infinite continuum.

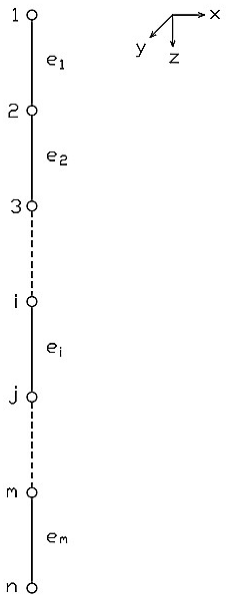

Figure 3. Nodes and elements of the embedded line load.

Equation (10) can be organized in matrix form for numerical implementation purposes, as discussed in the next section:

$$\{u\} = [G]\{Q\}. \tag{11}$$

The line load, as shown in Fig. 3, is discretized into m linear boundary elements. Only one component of displacement is considered for the purpose of illustrating the composition of matrix $[G]$ of the soil's influence coefficients. After performing the numerical integration, $[G]$ is obtained as shown in Eq. (12). The full matrix $[G]$ implemented in the computational code is a $3n \times 3n$ matrix, where n is the number of DOFs of a given model.

$$[G] = \begin{bmatrix} c_{11}^{e_1} & c_{12}^{e_1+e_2} & c_{13}^{e_2+e_3} & \dots & c_{1i}^{e_{i-1}+e_i} & c_{1j}^{e_i+e_{i+1}} & \dots & c_{1m}^{e_{m-1}+e_m} & c_{1n}^{e_n} \\ c_{21}^{e_1} & c_{22}^{e_1+e_2} & c_{23}^{e_2+e_3} & \dots & c_{2i}^{e_{i-1}+e_i} & c_{2j}^{e_i+e_{i+1}} & \dots & c_{2m}^{e_{m-1}+e_m} & c_{2n}^{e_n} \\ c_{31}^{e_1} & c_{32}^{e_1+e_2} & c_{33}^{e_2+e_3} & \dots & c_{3i}^{e_{i-1}+e_i} & c_{3j}^{e_i+e_{i+1}} & \dots & c_{3m}^{e_{m-1}+e_m} & c_{3n}^{e_n} \\ \dots & \dots & \dots & \dots & \dots & \dots & \dots & \dots & \dots \\ c_{i1}^{e_1} & c_{i2}^{e_1+e_2} & c_{i3}^{e_2+e_3} & \dots & c_{ii}^{e_{i-1}+e_i} & c_{ij}^{e_i+e_{i+1}} & \dots & c_{im}^{e_{m-1}+e_m} & c_{in}^{e_n} \\ c_{j1}^{e_1} & c_{j2}^{e_1+e_2} & c_{j3}^{e_2+e_3} & \dots & c_{ji}^{e_{i-1}+e_i} & c_{jj}^{e_i+e_{i+1}} & \dots & c_{jm}^{e_{m-1}+e_m} & c_{jn}^{e_n} \\ \dots & \dots & \dots & \dots & \dots & \dots & \dots & \dots & \dots \\ c_{m1}^{e_1} & c_{m2}^{e_1+e_2} & c_{m3}^{e_2+e_3} & \dots & c_{mi}^{e_{i-1}+e_i} & c_{mj}^{e_i+e_{i+1}} & \dots & c_{mm}^{e_{m-1}+e_m} & c_{mn}^{e_n} \\ c_{n1}^{e_1} & c_{n2}^{e_1+e_2} & c_{n3}^{e_2+e_3} & \dots & c_{ni}^{e_{i-1}+e_i} & c_{nj}^{e_i+e_{i+1}} & \dots & c_{nm}^{e_{m-1}+e_m} & c_{nn}^{e_n} \end{bmatrix} \tag{12}$$

The entry $c_{ij}^{e_k+e_l}$ is computed summing the influence coefficients at node j common to elements e_k and e_l, with the source point placed at node i.

4 Pile–Soil assembly equations

The final system of equations is obtained by coupling the pile equations with the soil equations, described in the previous sections. In this section, the subscripts 'p' and 's' refer to 'pile' and 'soil', respectively.

The pile's system of equations, as in Eq. (5), are:

$$[K_p]\{u_p\} = \{F\} + [T_p]\{Q_p\}. \tag{13}$$

The soil's system of equations, as in Eq. (11), are:

$$\{u_s\} = [G]\{Q_s\}. \tag{14}$$

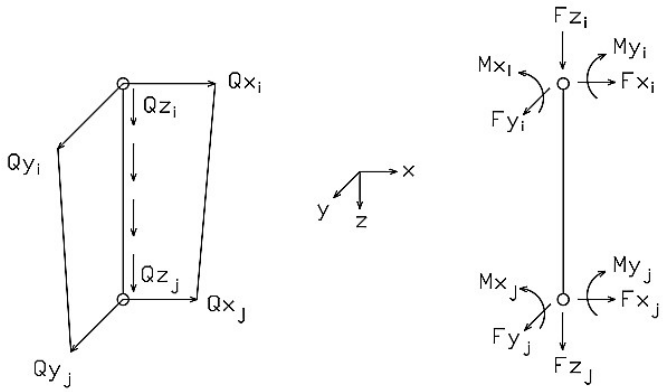

Figure 4. Tractions transformed into equivalent nodal forces.

The vector of equivalent nodal forces, considering a single finite element of the pile, is given as in Eq. (15), where $[T_p]^e$ is the transformation matrix and L is the length of the finite element.

$$\begin{pmatrix} F_{xi} \\ F_{yi} \\ F_{zi} \\ M_{xi} \\ M_{yi} \\ F_{xj} \\ F_{yj} \\ F_{zj} \\ M_{xj} \\ M_{yj} \end{pmatrix} = [T_p]^e \begin{pmatrix} Q_{xi} \\ Q_{yi} \\ Q_{zi} \\ 0 \\ 0 \\ Q_{xj} \\ Q_{yj} \\ Q_{zj} \\ 0 \\ 0 \end{pmatrix} \tag{15}$$

With the inverse of $[G]$, Eq. (14) can be rewritten as:

$$\{Q_s\} = [G]^{-1}\{u_s\}. \tag{16}$$

The force equilibrium must be verified along the pile–soil interface region, so that:

$$\{Q_s\} + \{Q_p\} = 0. \tag{17}$$

Equations (13) and (16) combined result in:

$$\left[K_p\right]\{u_p\} = \{F\} - [M]\{u_s\}. \tag{18}$$

Where:

$$[M] = \left[T_p\right][G]^{-1}. \tag{19}$$

Taking into account the displacement compatibility:

$$\{u_s\} = \left\{u_p\right\} = \{\bar{u}\}. \tag{20}$$

Equation (20) in Eq. (18) yields:

$$\left[\left[K_p\right] + [\bar{M}]\right]\{\bar{u}\} = \{F\}. \tag{21}$$

Where $[\bar{M}]$ is matrix $[M]$ augmented to have the same dimension of matrix $\left[K_p\right]$.

Finally,

$$[\bar{K}]\{\bar{u}\} = \{F\}. \tag{22}$$

$[\bar{K}]$ is the pile–soil assembly stiffness matrix and $\{\bar{u}\}$ is the vector encompassing all the nodal displacements and rotations of the assembly.

5 Results and discussion

Fortran® is the programming language used for the computational code implemented in a 64-bit Windows® environment, in an Intel® CPU 3.10 GHZ with 8 GB of RAM. The pile is meshed with 20 three-dimensional finite beam elements. The processing times, by order of the following examples, are 0.047 s (1 pile), 0.109 s (2 piles), 15.9 s (9 piles) and 0.594 s (4 piles).

5.1 Pile subjected to horizontal and bending moment loads

This example is based on the experiment performed by Kérisel and Adam (1967) in which an isolated pile, $L_p = 4.65\ m$ and $D_p = 0.3573\ m$, is driven into a clay soil, as shown in Fig. 5. The pile is subjected to horizontal load $H_x = 60\ kN$ and bending moment $M = 69\ kNm$. The Young's modulus of the pile is $2.0 \times 10^7\ kN/m^2$, and of the soil, $9233\ kN/m^2$ (measured experimentally), while Poisson's ratio of the soil is 0.3.

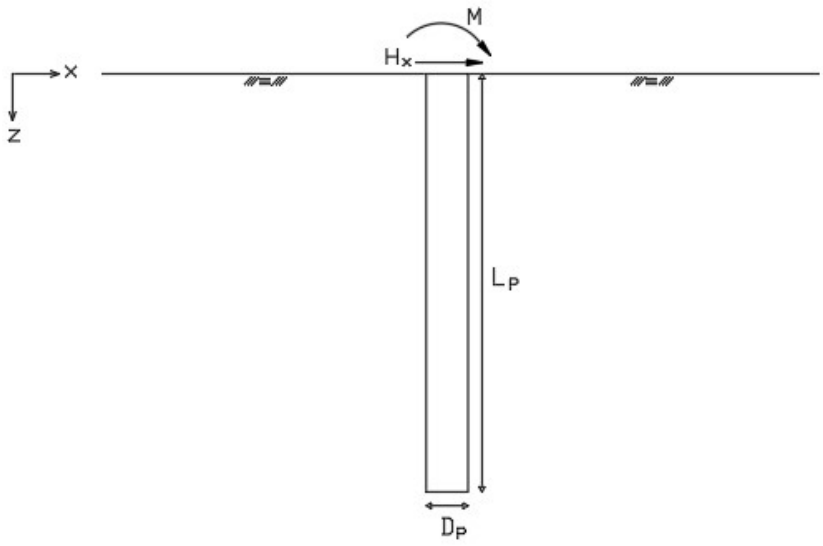

Figure 5. Pile subjected to horizontal and bending moment loads.

Figure 6 shows the calculated horizontal displacements along the pile and those obtained by Kérisel and Adam (1967). The numerical results agree well with the experimental results.

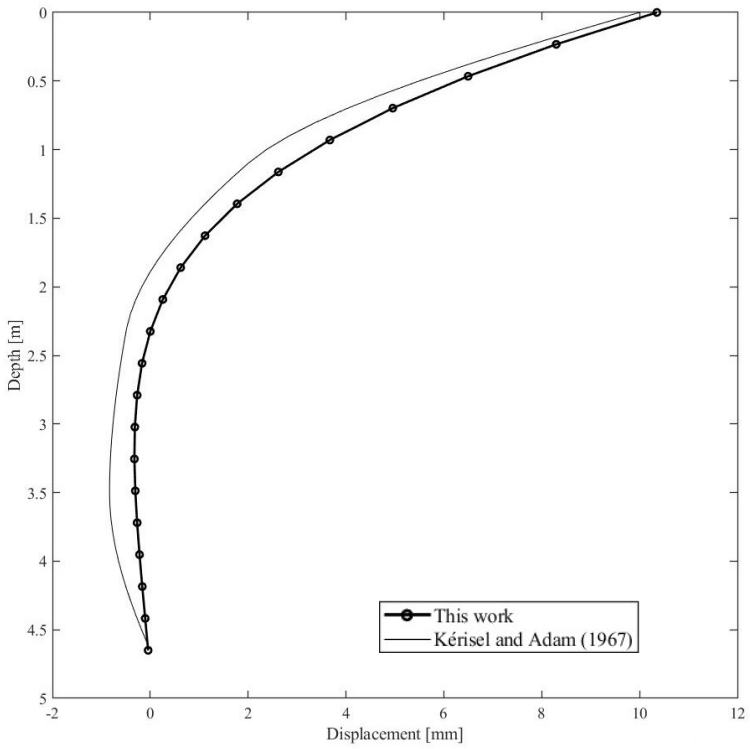

Figure 6. Comparison between numerical and experimental solutions.

By analyzing the problem by a FEM/FEM discretization, even taking advantage of the problem symmetry, the number of nodes is more than 100 times as many as the number of nodes required by a BEM/FEM discretization, as shown in Fig. 7. Moreover with the BEM/FEM approach and using Mindlin's fundamental solution, the boundary conditions for the remote regions are automatically satisfied.

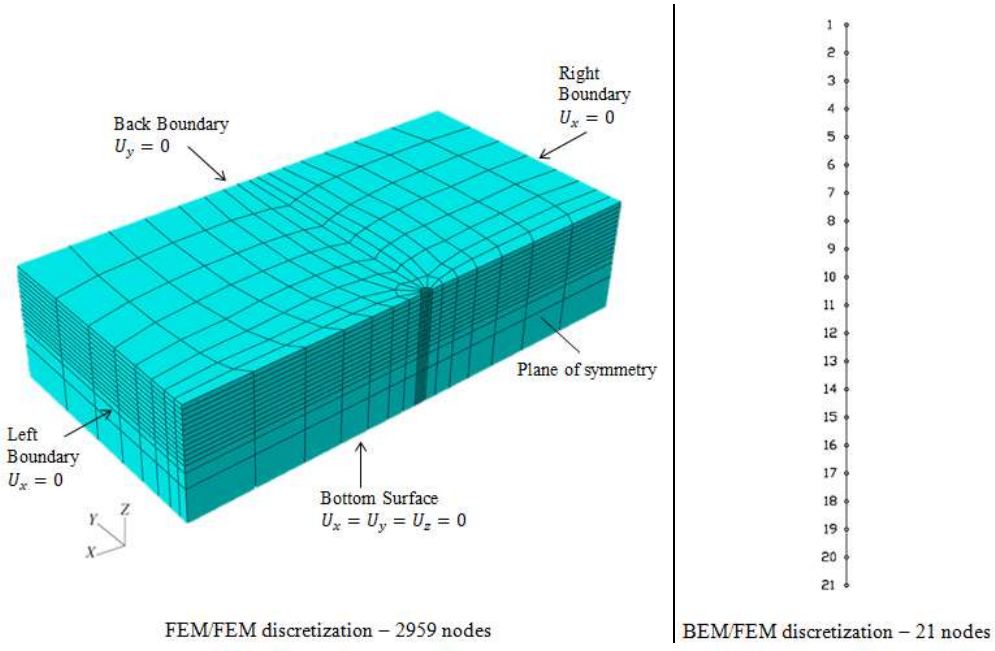

Figure 7. Pile–soil discretization using FEM/FEM (adapted from Helwany [2]) and BEM/FEM.

5.2 Pile subjected to horizontal and vertical loads

A pile of length $L_P = 25$ is embedded in a semi-infinite continuum with Poisson's ratio $\nu = 0.5$, as shown in Fig. 8. A unit load is applied to the top of the pile at the ground level. The pile flexibility factor is $K_R = 10^{-5}$ for a flexible pile and $K_R = 10$ for a rigid pile.

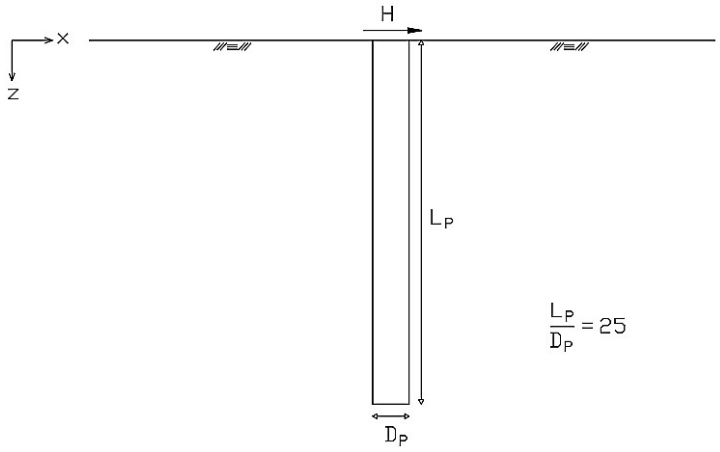

Figure 8. Pile subjected to horizontal load.

K_R is given by $K_R = \frac{E_P I_P}{E_S {L_P}^4}$.
$E_P I_P$ is the pile bending stiffness, L_P is the pile length, and E_S is the Young's modulus of the soil.

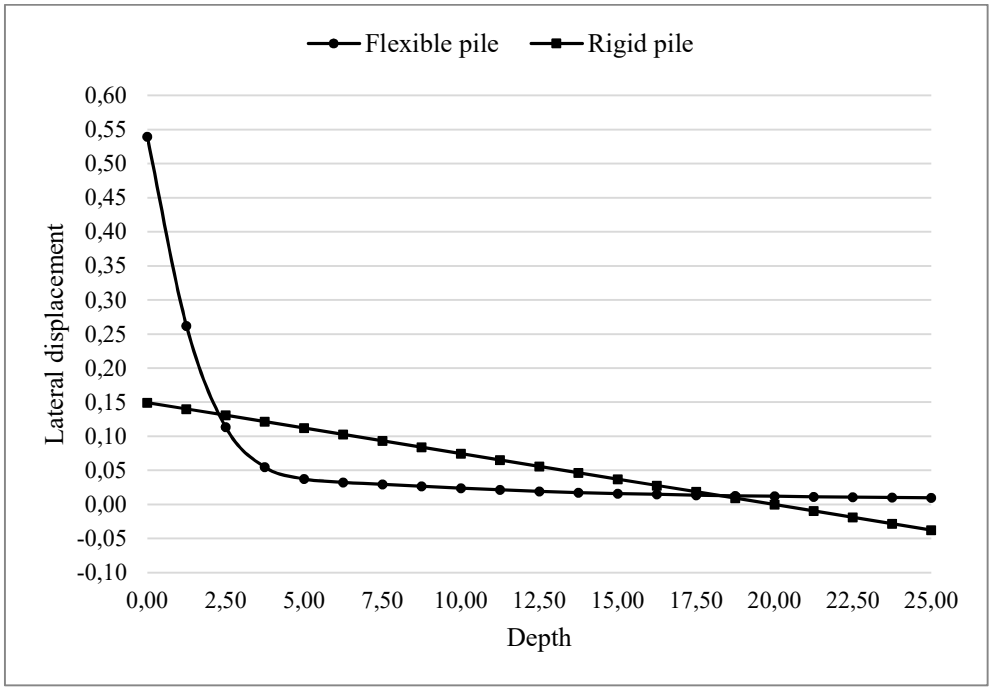

Figure 9. Influence of the rigidity on a laterally loaded pile.

It can be observed in Fig. 9 that for a flexible pile, the bending is mainly predominant in the upper part of the pile. From the half of the pile to the bottom, the bending is very slight, with very small and almost constant displacements. On the other hand, for a rigid pile, as expected, the displacements present a linear distribution along the depth. The results obtained are highly consistent with those presented in Parreira and Varatojo [4].

The pile can also be subjected to a unit vertical load and its vertical displacement, considering both a flexible and a rigid pile, is shown in Fig. 10. For a rigid pile, the displacement is constant along the depth.

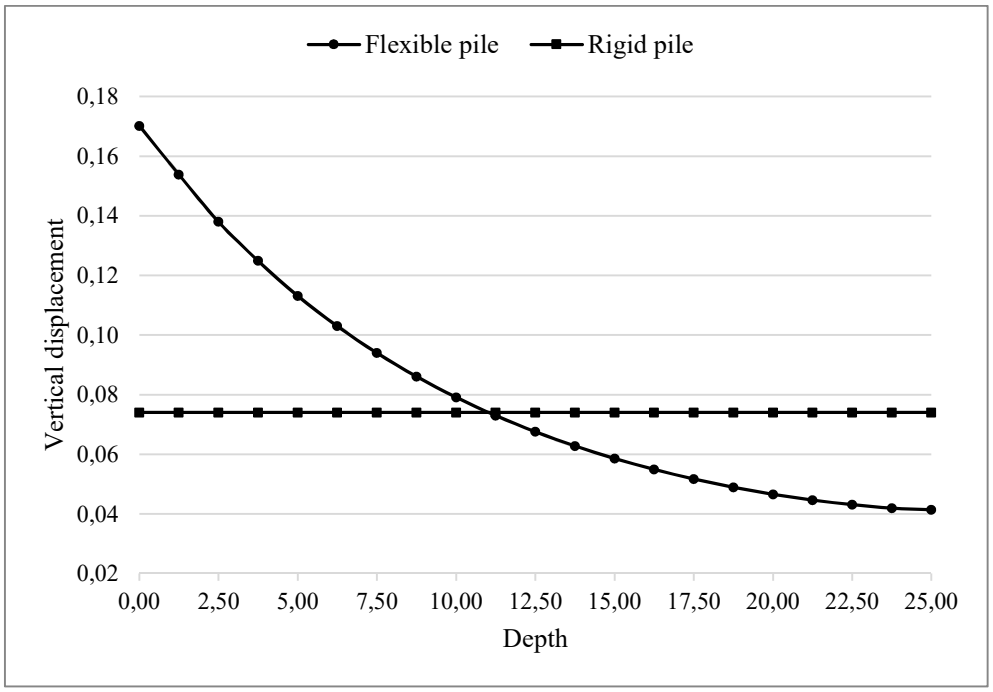

Figure 10. Influence of the rigidity on an axially loaded pile.

With the same data and considering a flexible pile, the influence of the spacing s between two piles, as shown in Fig. 11, is now analyzed.

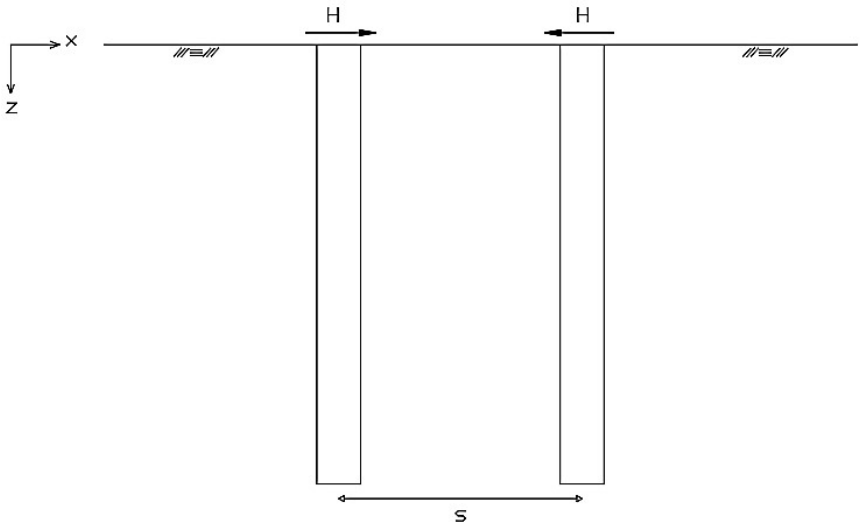

Figure 11. Two piles separated by a distance s.

In Fig. 12, where D is the pile diameter, it can be observed that the smaller the spacing between the piles, the more rigid the pile–soil assembly becomes, that is, the lateral displacement decreases. On the other hand, the interaction effects decrease as the spacing between the piles increases, resulting in the case of a single pile. In fact, as s increases in this example, the lateral displacement tends towards the one shown in Fig. 9 for a single flexible pile.

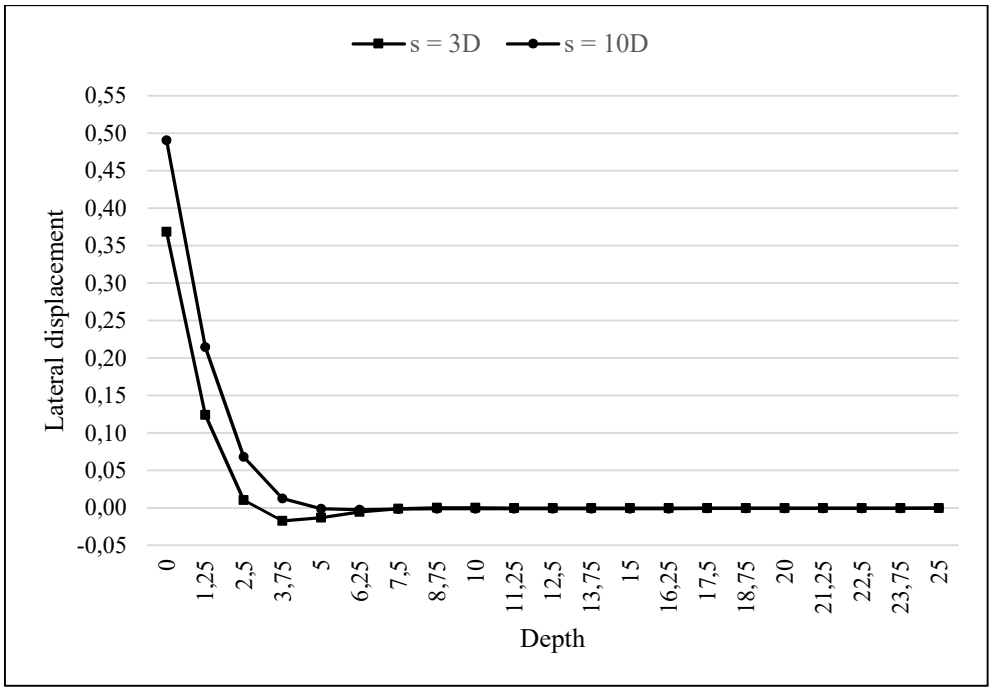

Figure 12. Influence of the spacing on a two-pile group.

5.3 Pile group subjected to horizontal loads

In this example, a group of 9 piles equally spaced and each subjected to horizontal load $H_x = 20\ kN$, is embedded in a semi-infinite continuum, as shown in Fig. 13. The pile group is divided into 4 subgroups considering the symmetry of the problem. Each pile has $L = 15\ m$, $D = 0.35\ m$ and $E_p = 1.0 \times 10^7\ kN/m^2$. The soil properties are $E_s = 1.0 \times 10^3\ kN/m^2$ and $\nu_s = 0.2$. The spacing between the piles' axes, both vertically and horizontally, is $s = 1.50\ m$.

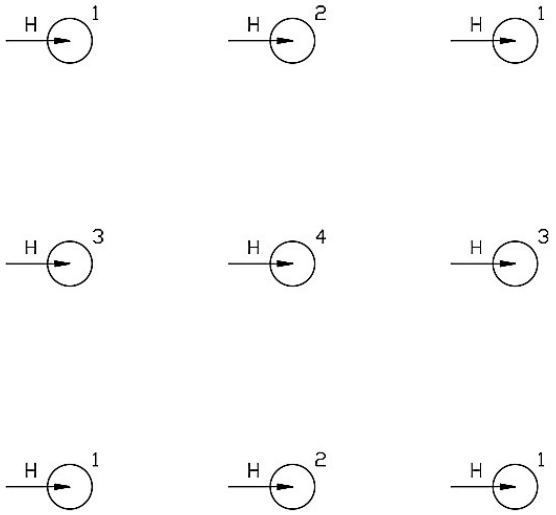

Figure 13. Group of 9 piles subjected to horizontal loads.

Table 1. Horizontal displacements at the top of the piles (mm)

Subgroup	This work	Matos Filho et al. [10]	Ribeiro and Paiva [3]
1	36.156	32.946	33.278
2	39.094	35.284	35.622
3	39.474	35.842	36.162
4	42.987	38.632	38.907

It can be observed in Table 1 that the smallest displacements occur in the piles located far from the geometric center (Subgroup 1) and the largest ones in the piles near the geometric center (Subgroup 4). Because the pile is relatively long and the load being horizontal, the discrepancy observed in the results is mainly due to the pile discretization assumed in each formulation. In the formulations presented in Matos Filho et al. [10] and Ribeiro and Paiva [3], the pile is modeled using a single finite element with four nodes. The formulation of this work allows for a better simulation of the flexibility of the pile discretized with twenty 3D finite beam elements, and comparing with the meshes presented in Parreira and Varatojo [4] and Ribeiro and Paiva [3], the one of the present study is highly practical.

5.4 Pile group subjected to horizontal loads in two directions

A pile group, as shown in Fig. 14, has four piles equally spaced and each subjected to horizontal loads H in both the x and y directions; the overall loading in the group is symmetrical so that equal displacements in modulus are expected. The problem data are all displayed in the figure.

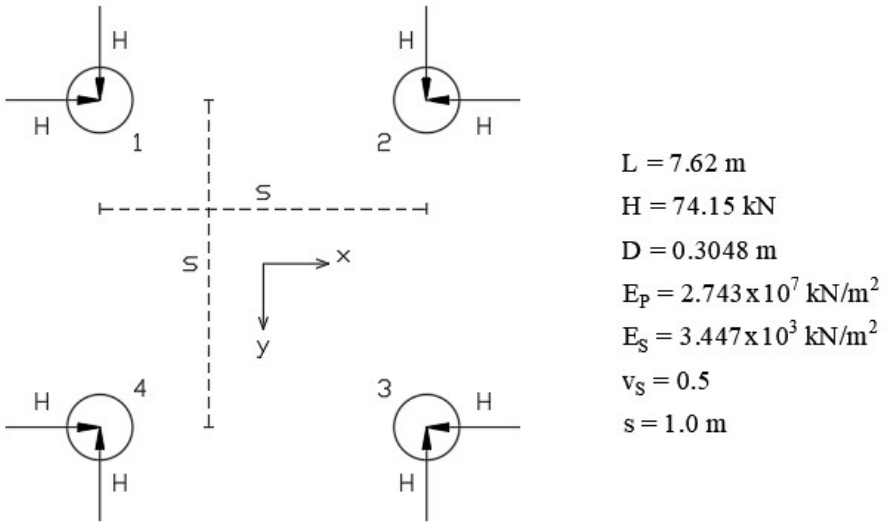

Figure 14. Group of 4 piles subjected to horizontal loads in two directions.

The displacements and rotations in Table 2 are given in modulus in order to simplify the table. The signal of the displacements in each direction corresponds to the signal of the applied load in that direction. For example, the displacements of pile 1, U_x and U_y, are both positive; for pile 2, U_x is negative and U_y is positive. In addition, at the top of each pile, U_x and θ_y, as well as U_y and θ_x, have opposite signs. θ_x and θ_y are rotations around the x-axis and y-axis respectively, and are positive counterclockwise.

Table 2. Horizontal displacements and rotations at the top of a pile

Displacements and rotations
$\|U_x\|$ = 9.21 mm
$\|U_y\|$ = 9.21 mm
$\|\theta_x\|$ = 6.52 ×10^{-3} rad
$\|\theta_y\|$ = 6.52 ×10^{-3} rad

Variations to the problem can be made in order to verify the influences of the length and diameter of the piles. The results are shown in Fig. 15 for the following combinations: (L,D), (L,2D), (2L,D) and (2L,2D). It can be seen that doubling the pile diameter has greater influence than doubling the pile length on the lateral displacements of the piles. Conversely, when the applied load is vertical, the pile length has greater influence in reducing the total settlement as a result of a larger shaft friction.

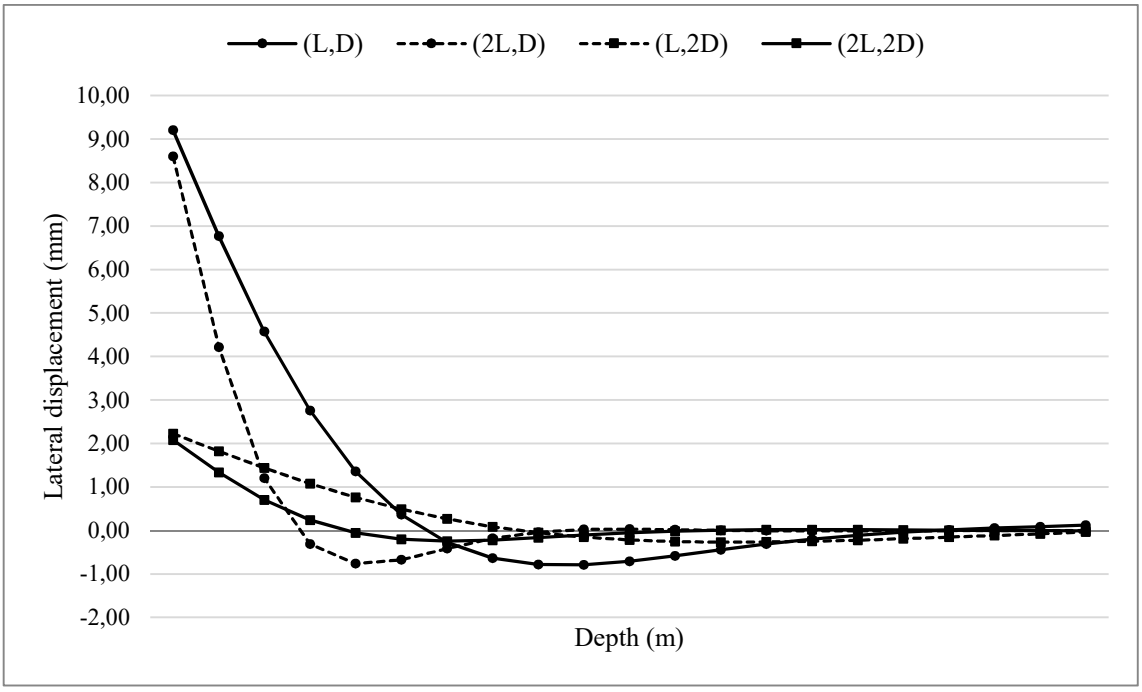

Figure 15. Influence of the length and diameter considering one pile of the pile group.

6 Conclusions

This paper presented a new formulation obtained by coupling BEM and FEM equations for an efficient analysis of single piles and pile groups interacting with the soil. The pile can be modeled by a parametric number of three-dimensional finite beam elements. In the examples presented, each pile is discretized into twenty elements to well account for the flexibility. The soil, on the other hand, is modeled with line loads using Mindlin's fundamental solution, resulting in a very practical mesh for the pile–soil assembly. In fact both the soil and the pile are modeled using the same discretization. Therefore, the analysis is very efficient in terms of processing time and problem modeling. The effects of parameters like pile's rigidity, pile's dimensions and spacing between piles have been properly quantified. The results obtained with the proposed BEM/FEM coupling formulation are in good agreement with those from other formulations. In future formulations, the authors intend to consider a multi-layered soil and the pile may slide along the pile–soil interface region.

Acknowledgements

This study was financed in part by the Coordenação de Aperfeiçoamento de Pessoal de Nível Superior - Brasil (CAPES) - Finance Code 001.

References

[1] Kérisel J., Adam M. Calcul des forces horizontales applicables aux fondations profondes dans les argiles et limons. *Les Annales de l'ITBTP*, Paris, France, n. 239, pp. 1653–1694, 1967.
[2] Helwany S. *Applied soil mechanics with ABAQUS applications*. John Wiley & Sons, Inc., Hoboken, New Jersey, 2007.
[3] Ribeiro D.B., Paiva J.B. A new BE formulation coupled to the FEM for simulating vertical pile groups. *Engineering Analysis with Boundary Elements*, vol. 41, pp. 1–9, 2014.
[4] Parreira P., Varatojo P. 3D boundary element discretizations for linear elastic analysis of flexible and rigid piles. *Transactions on Modelling and Simulation*. WIT Press, vol. 3, pp. 217–227, 1993.
[5] Aliabadi M.H. *The Boundary Element Method: Applications in Solids and Structures*. John Wiley & Sons, Inc., Chichester, West Sussex, vol.2, pp. 1–5, 2002.
[6] Luamba E.S., Paiva J.B. A BEM/FEM formulation for the analysis of piles submitted to horizontal loads. *Engineering Analysis with Boundary Elements*, vol. 81, pp. 12–20, 2017.
[7] Mindlin R.D. Force at a point in the interior of a semi-infinite solid. *Physics*, vol. 7, pp. 195–202, 1936.
[8] Poulos H.G., Davis EH. *Pile foundation analysis and design*. John Wiley & Sons, New York, 1980.
[9] Ai Z.H., Feng D.L., Cheng Y.C. BEM analysis of laterally loaded piles in multi-layered transversely isotropic soils. *Engineering Analysis with Boundary Elements*, vol. 37, pp. 1095–1106, 2013.
[10] Matos Filho R., Mendonça A.V., Paiva J.B. Static boundary element analysis of piles submitted to horizontal and vertical loads. *Engineering Analysis with Boundary Elements*, vol. 29, pp. 195–203, 2005.